The Decarburization Kinetics of Metal Droplets in Emulsion Zone

AMEYA KADROLKAR and NESLIHAN DOGAN

A mathematical model has been developed to predict the decarburization rate within individual droplets in the emulsion zone. All the chronological events pertaining to the life cycle of a metal droplet in the emulsion zone like oxygen supply (from slag), external and internal decarburization have been modeled dynamically and validated against experimental data available in open literature. The bloating behavior of metal droplets in the emulsion was represented theoretically by incorporating an escape function dependent on internal CO gas generation. The model is able to predict the onset of bloating and the residence time of metal droplets in the emulsion zone. The residence time of droplet containing 2.6 wt pct C and 0.007 wt pct S is in the range of 10 to 13 seconds. The contribution of decarburization rate in the emulsion zone to the overall decarburization rate is studied using the industrial data reported by Cicutti et al. The model predicts 5 to 75 pct of total decarburization takes place in the emulsion zone. It is found that the extent of decarburization of a metal droplet depends on its initial carbon content rather than its oxygen content for slag containing FeO greater than 10 wt pct.

I. INTRODUCTION

IN oxygen steelmaking, large number of metal droplets are generated and ejected into the slag due to the high speed oxygen jet impingement on the metal bath.[1,2] This leads to the formation of a large interfacial area between the metal droplets and the slag and enhances the kinetics of the refining reactions during oxygen blow. Few studies[1–6] investigated the contribution of refining reactions in the emulsion zone by sampling metal droplets from pilot plant trials. Meyer et al.[1] quantified the number of droplets generated in the emulsion zone and predicted the residence time of these droplets in order to investigate the refining rates in the emulsion zone. It was found that instantaneous carbon content of droplets in the emulsion were lower than that of bath[1] thus establishing the emulsion zone as a significant contributor to the decarburization reaction. Similar findings were reported by other researchers.[3,6] These industrial findings motivated several researchers[7–14] to study the behavior of a single metal droplet in a slag for a more fundamental understanding of reaction kinetics between metal and slag. Mulholland et al.[7] pioneered the use of X-ray fluoroscopy to study the effect of metal droplet size, metal and slag compositions, and temperature on the decarburization behavior of droplets. The study provided valuable qualitative insight about formation of gas halo surrounding the metal droplet. Gaye and Riboud[9] firstly measured the reaction rate through measurement of flow rate of gas formed inside the chamber and came to be known as Constant Volume Pressure Increase (CVPI) technique. The combination of X-ray fluroscopy and CVPI technique aided the in situ observation and quantitative measurement of decarburization reaction.[10–12,14–16] This combination was firstly employed by Min and Fruehan[10] for studying the decarburization rate of a metal droplet reacting with slags containing less than 10 wt pct FeO and suggested a 'mixed control model' for emulsion zone decarburization. Later, using similar set-up, Molloseau and Fruehan[11] observed that the decarburization rate of droplets ([C] = 2.9 wt pct) in contact with slags with (FeO) > 10 wt pct 'emulsified'. The CO evolution from the metal droplets (with similar carbon content) was found to be dependent on the FeO content in slag. Similar technique was used for Coley and his co-workers[12,14,17] to further study the decarburization kinetics under various conditions relevant to steelmaking operations. Chen and Coley[12] focussed on the effect of droplet size, FeO content in the slag and temperature on internal CO gas generation rates and bloating behavior. They proposed a model to predict the rate of internal CO gas generation. Homogeneous nucleation of CO gas

AMEYA KADROLKAR and NESLIHAN DOGAN are with the McMaster Steel Research Centre, McMaster University, JHE 357, 1280 Main Street West, Hamilton, ON L8S 4L7, Canada. Contact e-mail: kadrola@mcmaster.ca

bubbles within the metal droplet in ferruginous slag has been found to be responsible for bloating of droplets (leading to reduction of its density) and extending its residence time in the slag–gas–metal emulsion. Pomeroy and Coley[14] conducted further experimental study to identify the time for onset of bloating of the droplet due to internal CO gas generation. Recent study by Gu et al.[15] focussed on the dephosphorization kinetics using similar experimental set-up. They suggested that the internal stirring induced by the CO bubbles accelerates the refining of phosphorus and is expected to have similar effect on refining of silicon and manganese.

There are few proposed mathematical models[18–24] which incorporate the insights from experimental studies to predict the refining kinetics within metal droplets and its importance to the overall process kinetics. In the model proposed by Sun and Zhang,[18] the effect of Si and Mn on the decarburization kinetics was included. However, the nucleation of CO bubbles is assumed to occur on the surface of a metal droplet and while the CO nucleation within the metal droplet is not considered. Brooks et al.[24] developed a mathematical model to predict the trajectory of a metal droplet using ballistic motion. The rate determining mechanism of decarburization reaction was assumed to be carbon diffusion in a metal droplet. This model was applied by Dogan et al.[19,20] for quantifying the decarburization in the emulsion zone. This model was further expanded by Rout et al.[22,23] to incorporate the modified droplet generation rate and site blockage/poisoning effect of the surface activity of (SiO_2), (P_2O_5) and [S] on the decarburization reaction. They have incorporated the refining rates of other impurities and able to predict the slag formation path during oxygen blowing process. But the mechanism of the decarburization reaction is almost similar to that of Dogan et al.[19,20] Further the surface blockage effect of (SiO_2) is likely to be over-estimated since the effect of (CaO) is not considered. Sarkar et al.[21] quantified the refining rates within the emulsion zone by distributing the oxygen amongst decarburization and other refining reactions based on the free energy minimization technique. However, this methodology does not consider the CO generation inside the metal droplets. Additionally, the residence time of metal droplet is assumed to equal total time elapsed when the maximum possible decarburization of droplet takes place. This condition is not necessarily true as the decarburization might be interrupted by insufficient residence time of droplet in the emulsion.

Although these models have incorporated some insights from experimental data, a recent finding on bloating of droplet due to internal CO generation has not been successfully applied to describe the decarburization kinetics in the emulsion zone. The current work aims to provide better knowledge on the decarburization rate within the droplets under full scale operating conditions at high temperatures. This model is based on a more mechanistic description of the droplet–slag behavior by incorporating the internal and external CO gas generation rate as well as its escape rate within metal droplets. The model was validated against available experimental studies and industrial data. In the present study, the effects of temperature and oxygen content of metal droplet on the decarburization rate in the emulsion zone are studied.

II. MODEL DEVELOPMENT

The theoretical treatment suggested by Dogan et al.[20] is applied in this study to predict total decarburization rate in the emulsion zone. This rate can be calculated by the summation of decarburization rates of individual metal droplets for a given time using the following equation.

$$\frac{dW_C}{dt} = \frac{\sum_{i=1}^{n} \frac{m_d}{100}\left(C_i^{t+\Delta t_e} - C_i^t\right)}{\Delta t_e} \qquad [1]$$

where C_i^t and $C_i^{t+\Delta t_e}$ are the carbon contents of a single metal droplet entering and leaving the emulsion zone (wt pct), respectively. m_d is the mass of a single droplet (kg) and n is the total number of droplets generated at a defined time interval Δt_e. Time interval is chosen to be 1 second. In the model, the droplet generation rate is calculated using blowing number proposed by Subagyo et al.[25] It should be noted that the calculation approach for residence time of droplets has been changed. The residence time of droplets is strongly dependent upon the apparent density of droplets in comparison to the density of slag–metal–gas emulsion. The dynamic changes in the droplet's density can be calculated when net CO gas within a single droplet is known. The modeling of aspects pertaining to the calculation of net CO gas within the metal droplet, namely supply of oxygen (from slag), internal and external CO gas generation and escape of CO gas from the droplet are described below.

A. Oxygen Supply

The supply of oxygen for the refining reactions in emulsion zone comes from FeO in the slag and described by the following reaction at the metal droplet surface,

$$(FeO) = [Fe] + [O] \qquad [2]$$

The FeO flux, J_{FeO} (mol/s) through the slag due to the above reaction can be written as per the mass transfer model suggested by Min and Fruehan,[10]

$$J_{FeO} = \frac{A_d k_s \rho_s}{100 M_{FeO}} (FeO - FeO^r) \qquad [3]$$

where J_{FeO} is the oxygen atoms at the metal surface, moles/s, A_d is the area of a droplet, m^2, k_s is the slag phase mass transfer coefficient, $\frac{m}{s}$, and M is the molecular weight of individual component, $\frac{g}{mol}$, FeO and FeO^r are the concentrations of FeO in slag bulk and droplet–slag interface, respectively, in wt pct.

This mass transfer model does not account for the non-equilibrium caused by the surface activity of sulfur. In order to include this effect, Min and Fruehan's model[10] is modified by considering non-equilibrium

FeO dissociation reaction at the surface due to sulfur concentration, and the equation can be represented by difference between the forward $\bar{k}$ and backward $\bar{\bar{k}}$ reaction for the FeO dissociation reaction (Eq. [2]). This approach was originally suggested by Pomeroy[14] and is applied in the current study

$$J_{\text{FeO}} = A_{\text{d}}(1 - \theta_{\text{S}})\left[\bar{k}a^r_{\text{FeO}} - \bar{\bar{k}}h^r_{\text{O}}\right] \qquad [4]$$

where a^r_{FeO} and h^r_{O} are the activities of FeO and O at the interface, respectively. θ_{S} is the fraction of surface area unavailable for reaction due to poisoning by sulfur and is calculated using the correlation suggested by Belton.[26]

$$\theta_{\text{S}} = \frac{K_{\text{s}}h_{\text{s}}}{1 + K_{\text{s}}h_{\text{s}}} \qquad [5]$$

where K_{s} is the adsorption coefficient of sulfur, and its evaluation is explained further in subsequent section.

The forward and backward reaction constants can be related to the equilibrium constant by the following relation,

$$K_{\text{FeO}} = \bar{k}/\bar{\bar{k}} \qquad [6]$$

where K_{FeO} is the equilibrium constant for FeO dissociation reaction (Eq. [2]) and is given by the following equation[27]

$$K_{\text{FeO}} = 10^{\left(\left(\frac{6150}{Td}\right) - 2.604\right)} \qquad [7]$$

The Eqs. [4] and [6] can be combined to arrive at the following equation

$$J_{\text{FeO}} = \bar{k}A_{\text{d}}(1 - \theta_{\text{S}})\left(a^r_{\text{FeO}} - \frac{h^r_{\text{O}}}{K_{\text{FeO}}}\right) \qquad [8]$$

The Eqs. [3] and [8] are combined to arrive at the following equation

$$\bar{k}A_{\text{d}}(1 - \theta_{\text{S}})\left[a^r_{\text{FeO}} - \frac{h^r_{\text{O}}}{K_{\text{FeO}}}\right] = \frac{A_{\text{d}}k_{\text{s}}\rho_{\text{s}}}{100M_{\text{FeO}}}(\text{FeO} - \text{FeO}^r) \qquad [9]$$

The values of the three interfacial terms Eq. [9] (a^r_{FeO}, h^r_{O} and FeO^r) are obtained by the solving Eq. [9] and other non-linear Eqs. [18] and [21] from subsequent section and Appendix A ([A1] through [A6] and [A9]). With the knowledge of value of FeO^r the net supply of oxygen can be calculated from Eq. [3] at each time step.

B. Decarburization Reaction

The supplied oxygen reacts with carbon within the metal droplet and forms carbon monoxide (CO) gas,

$$[\text{C}] + [\text{O}] = \text{CO} \qquad [10]$$

This reaction could either happen at the surface of the metal droplet (heterogeneous nucleation) or within the droplet (homogeneous nucleation/internal decarburization). The equilibrium constant, K_{CO} for this reaction

is given by the following equation,[28]

$$\log K_{\text{CO}} = \frac{1160}{T} + 2 \qquad [11]$$

where,

$$K_{\text{CO}} = \frac{P_{\text{CO}}}{h_{\text{C}}h_{\text{O}}} \qquad [12]$$

where P_{CO} is the supersaturation pressure of the CO bubble nucleated, h_{C} and h_{O} are the Henrian activities of carbon and oxygen in the metal droplet, respectively and calculated using the following equations.[28]

$$h_{\text{C}} = f_c[\text{C}] \qquad [13]$$

$$h_{\text{O}} = f_{\text{O}}[\text{O}] \qquad [14]$$

The activity of elements is calculated from the activity coefficients by using the following equations.

$$\log f_{\text{C}} = e^{\text{C}}_{\text{C}}[\text{C}] + e^{\text{O}}_{\text{C}}[\text{O}] + e^{\text{S}}_{\text{C}}[\text{S}] \qquad [15]$$

$$\log f_{\text{O}} = e^{\text{C}}_{\text{O}}[\text{C}] + e^{\text{O}}_{\text{O}}[\text{O}] + e^{\text{S}}_{\text{O}}[\text{S}] \qquad [16]$$

where $e^{\text{C}}_{\text{O}}, e^{\text{O}}_{\text{O}}$ and e^{S}_{O} are the first order interaction parameters, and obtained from the literature.[29] [·] represents the concentration of the element dissolved in the bulk metal droplet (wt pct). The activities of elements are calculated as a function of instantaneous composition of metal droplet. This step is critical because change in the amount of a given metal component causes considerable change in the activities of other components. For instance, the activity of sulfur decreases as the carbon content of the droplet decreases because carbon has a positive interaction parameter with respect to sulfur. The activity of sulfur will further affect its surface tension and rate of the reactions at droplet–slag interface.

C. External Decarburization

External decarburization was studied by few researchers.[10,18] In their high temperature experiments, they used low FeO containing slags in order to ensure that external decarburization occurred predominantly. Min and Fruehan[10] examined the effect of FeO content in the slag and sulfur content in metal droplet on the decarburization reaction and proposed a 'mixed control model'. They considered that mass transfer in the slag, mass transfer in the gas halo and chemical reaction at metal droplet–slag interface either partially or entirely controlled the decarburization reaction depending on the sulfur content of metal droplet. Similarly, Sun and Zhang[18] conducted experiments to predict the behavior of single droplet in a slag containing 10 wt pct FeO at 1773 K and further modeled the droplet–slag reactions by solving a set of non-linear equations pertaining to molar fluxes of components in metal and slag, interfacial activities of metal and slag components and interfacial

reaction equilibria. This model incorporates possible control mechanisms except the poisoning effect of sulfur. In current study the external decarburization is calculated using the approach adapted from the work of Sun and Zhang[18] but the poisoning effect of sulfur on the metal–slag interfacial is also incorporated (based upon approach suggested by Pomeroy[14]). Accordingly the rate of external decarburization, J_{ext} can be stated as

$$J_{ext} = \frac{(1 - \theta_S)k_{ext}A_d}{100M_C}\left(h_C^r h_O^r - \frac{P_{CO}^{ext}}{K_{CO}}\right) \quad [17]$$

where k_{ext} is the rate constant of decarburization reaction and equals 0.0136, $\left(\frac{kg}{m^2 \cdot s}\right)$. This value is taken from literature.[14,30] h_C^r and h_O^r are the activities of carbon and oxygen at the droplet–slag interface, respectively. P_{CO}^{ext} is the supersaturation pressure of the CO bubble nucleating on the surface of the droplet and was assumed to be equal to the pressure inside the furnace (1.5 atm).

The flux of carbon towards the slag–metal interface (J_C) (mol/s)) is equal to the consumption of carbon by external decarburization

$$J_C = J_{ext} \quad [18]$$

where J_C is defined by Fick's first law as given in the following equation[18]:

$$J_C = \frac{A_d k_m \rho_m}{100M_C}([C] - [C]^r) \quad [19]$$

where k_m is the metal phase mass transfer coefficient of the elements (m/s). Its value is taken from the study of Shibata et al.[30] and equal to 1.5×10^{-5} m/s. ρ_m is the density of metal droplet $\left(\frac{kg}{m^3}\right)$, $[]^r$ represents the interfacial concentration of the element. Similarly the flux of oxygen towards the slag–metal interface, J_O is given by

$$J_O = \frac{A_d k_m \rho_m}{100M_O}([O] - [O]^r) \quad [20]$$

The supply of oxygen takes place from slag FeO of which a fraction is consumed by carbon and rest diffuses into the metal droplet to raise the oxygen concentration of the droplet, this balance is represented in the following equation:

$$J_O = J_C - J_{FeO} \quad [21]$$

D. Internal Decarburization

Although internal/homogeneous CO gas generation has been observed for metal droplets exposed to oxidizing gases[31–35] and slags,[11] only few studies[33,36–38] proposed a theoretical explanation for it. Recently, Chen and Coley[12,13] conducted X-ray fluoroscopy experiments at steelmaking temperatures and developed a mathematical model for internal nucleation rate of CO gas bubbles. Based on their experimental observations, Chen and Coley[12,13] modified the classical homogeneous nucleation rate equation by introducing a correction/modifying parameter 'ψ' to the surface tension of the metal droplet. This parameter physically represents the extent of decrease in energy barrier for homogeneous nucleation described differently by various authors.[36–38] Levine[36] suggested that this parameter accounted for the action of 'doubly charged oxygen ions' chemisorbed on CO embryos in lowering the surface tension. The decrease in surface tension in turn lowers the energy barrier for the nucleation. Bowers et al.[37] proposed a theory which involved formation of a metastable blob phase before the bubble nucleation. The interfacial energy between the blob and the solvent is considerably less than that for a bubble, which a sharp interface (and hence higher interfacial energy). This makes the nucleation possible at lower supersaturation levels than predicted by classical nucleation theory. Similarly Lubetkin[38] used the surface activity of gases (oxygen in current system) which lead to bubble formation to describe nucleation occurring at lower supersaturation than predicted by theory. The nucleation rate of CO gas in a metal droplet is given by the following equation[12]

$$J_s = N_o\left(\frac{3\psi\sigma}{\pi m}\right)^{\frac{1}{2}}\exp\left(-\frac{\Delta H}{kT}\right)\exp\left(-\frac{16\pi(\psi\sigma)^3}{3kT\left(\Delta P_{CO}^{int}\right)^2}\right) \quad [22]$$

where J_s is the nucleation rate, number of nuclei/m$^3 \cdot$s, σ is the surface tension of metal droplet, '$\psi\sigma$' represents the surface tension at liquid metal–CO gas interface due to oxygen ions, (N/m), ΔH is the heat of formation of one CO molecule; m is the mass of one molecule of CO gas, kg, T is temperature, K, k is Boltzman constant, J/K. N_o is the number concentration of CO embryos in the liquid and its value is calculated using the following equation

$$N_o = N_A \times \frac{n_O}{V_o} \quad [23]$$

where n_O is the moles of oxygen present in a metal droplet, V_o is the initial volume of metal droplet. As an embryo of CO is formed from carbon and oxygen, the number of concentration of CO embryos would depend on the smaller value amongst the concentrations of the two elements in liquid iron. In case of steelmaking, the activity of carbon in liquid iron is much higher than that of oxygen. Hence the value of N_o depends on oxygen concentration rather than that of carbon. ΔP_{CO}^{int} is the difference of CO vapor bubble pressure at equilibrium inside the metal droplet and pressure inside the furnace and can be calculated using Eq. [24].

$$\Delta P_{CO}^{int} = P_{CO} - P_{furnace} \quad [24]$$

The internal CO generation rate, J_{int} in mole/s can be represented as[12]

$$J_{\text{int}} = J_s \times \left(\frac{n_e}{N_A} \right) \times V_o \qquad [25]$$

where n_e is the number of molecules in a CO embryo, N_A is Avogadro number, V_o is the initial volume of metal droplet, m^3. To the best of authors' knowledge, this model can predict the internal nucleation rate of CO bubbles satisfactorily under the relevant oxygen steelmaking conditions and it has been used in the current work.

E. Surface Tension of Metal Droplet

The surface tension of the metal is a critical parameter affecting the instantaneous CO nucleation rate. The surface-active elements such as sulfur and oxygen have a negative effect on surface tension, whereas carbon has a positive effect. Previous studies[39–43] have examined the individual and combined effects of these elements. The equation suggested by Chung and Cramb,[44] is used in this study since it is the most comprehensive equation for calculating the surface tension of metal droplet incorporating effects of $[C], [S], [O]$ as well as temperature,

$$\begin{aligned} \sigma_{\text{metal}} = \ & 1913 + (67.75 \times [C]) + (0.43 \times (1813 - T)) \\ & - (0.107 \times T \times \ln(1 + (K_S h_S))) \\ & - (0.153 \times T \times \ln(1 + (K_O h_O))) \end{aligned}$$
$$[26]$$

where K_O and K_S are the adsorption coefficients of the oxygen and sulfur and calculated as follows[44]

$$\log K_O = \left(\frac{11370}{T} \right) - 4.09 \qquad [27]$$

$$\log K_S = \left(\frac{10013}{T} \right) - 2.87 \qquad [28]$$

The instantaneous changes of composition of droplet due to CO nucleation and oxygen diffusion are accounted for while calculating the surface tension of metal droplet. The decrease in surface tension due to $[S]$ and $[O]$ are derived from their surface activity due to their selective adsorption at the interface. Initially as the concentration of surface-active elements increases the surface activities increase leading to decrease in surface tension; however, beyond a certain concentration there is no increase in surface activity (or consequent decrease in surface tension). Halden and Kingery[45] firstly defined 'Excess surface concentrations' through use of Gibbs isotherm. They demonstrated that increase in excess surface concentration is observed with an increase in concentration of surface-active agent thus leading to decrease in surface tension. However beyond a particular activity/concentration excess surface concentration remains constant and the surface tension remains constant even if the concentration of surface-active agent is increased. Several studies[41,43] focused on the effect of oxygen concentration on the surface tension of liquid metal. The values ranged from 0.04 to 0.1. Similarly, the concentration of sulfur ranged from 0.02 to 0.1. Accordingly, in current calculations the maximum concentrations of O and S are set as 0.07 and 0.02 wt pct, respectively.

F. Escape Rate of CO Gas

The model predictions of internal CO gas generation profile and the corresponding escape rate profile are illustrated in Figures 1(a) and (b), respectively. These results are obtained for 1 g droplet reacting with slag at 1853 K from the study of Gu et al.[15] It can be seen in Figure 1(a) that the internal decarburization started at 2 seconds, and at this instant total CO gas generated increased its peak value leading to significant accumulation of CO gas thereby bloating of the droplet. In the meantime, CO gas exerted significant pressure on the walls of the droplet and started to escape from the droplet. The escape of gas from the droplet started at 5 seconds and peaked at 11 seconds as seen in Figure 1(b). The net outward force exerted on the CO bubbles at the droplet wall is a function of net CO gas present (or CO gas generation rate) inside the metal droplet as well as the surface tension of the metal droplet (a function of its composition). In the current work, a hyperbolic secant function was defined to generate the gas escape profile of a bloated droplet and is given by

$$J_{\text{esc}-t} = \left(\Delta t \times \sum J_{\text{int}} \right) \times \frac{1}{4} \times \sec h^2 \left(\frac{t - \mu}{2} \right) \qquad [29]$$

where $J_{\text{esc}-t}$ is the net escaped moles of CO gas at time instant 't', μ is location parameter of the function and its value is proportional to droplet diameter/size, $\mu \propto d_d$. The value of μ lies between 2 and 9 for droplet size ranging from 0.5 to 6×10^{-3} m.

The function is based on the study by Zhu and Coley.[46] They found that the CO gas escape rate profile strongly depends on the internal CO gas generation profile. To the best of authors' knowledge, this is the only study available in literature to predict the escape rate of CO gas from a metal droplet reacting with slags and it is used as basis of the current predictions of CO gas escape profile.

The net escaped moles of CO gas, $J_{\text{esc}-t}$ at a given time step are obtained from the escape rate profile and used to evaluate the net moles of CO gas retained inside a droplet, $N_{\text{CO}-t}$ at a given time step. The equation to calculate the net retained moles of CO gas within a metal droplet can be written as

$$N_{\text{CO}-t} = (J_{\text{int}-t} \times \Delta t) - J_{\text{esc}-t} + N_{\text{CO}-(t-1)} \qquad [30]$$

G. Residence Time of Metal Droplet

In the current study, the residence time of a droplet is defined as the time interval between the arrival of a single metal droplet in the emulsion and sinking back into the metal bath. The residence time depends upon
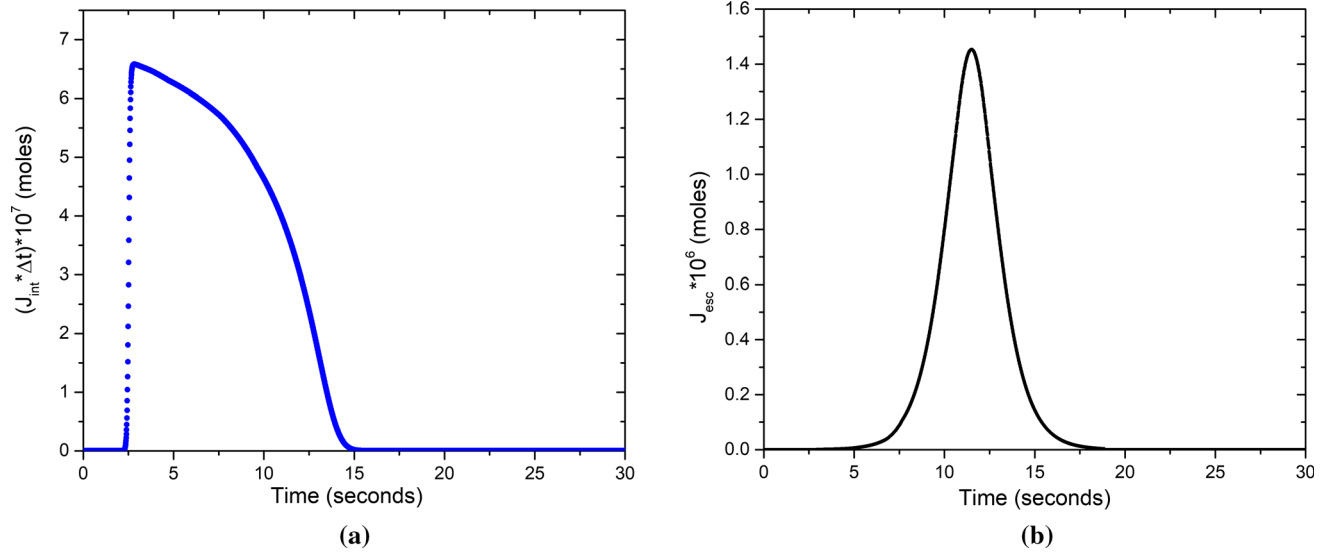
Fig. 1—Prediction of (a) internal CO gas generation and (b) corresponding escape rate for a 1 g droplet at 1853.15 K in slag.

the change in density of the metal droplet due to the existing CO gas within the droplet. The net moles of CO gas within the droplet is calculated using Eq. [30]. The instantaneous density of a single droplet is calculated using the following equation,

$$\rho_t = \frac{m_{dt}}{\left(\frac{m_{dt}}{\rho_d}\right) + \left(\frac{N_{CO-t} * M_{CO}}{\rho_{CO}}\right)} \quad [31]$$

where m_{dt} is the weight of metal droplet at given time instant, kg, ρ_d and ρ_t are the initial and apparent density of a metal droplet, respectively, $\frac{kg}{m^3}$. ρ_{CO} is the density of nucleated CO at the temperature equal to that of metal droplet. If the apparent density of the droplet is less than the density of emulsion, then the droplet is assumed to be suspended in the emulsion, else the droplet sinks back into the bath. The density of emulsion can be calculated using the following correlation[24,47]

$$\rho_{s-g} = \rho_g \phi_g + \rho_s (1 - \phi_g) \quad [32]$$

where ϕ_g is the volume fraction of CO gas in the emulsion and ρ_g and ρ_s are the gas and slag densities, respectively. In the current work, the volume fraction of CO gas in the emulsion is assumed to be constant and the value is taken to be 0.8. The slag density[20] is calculated by considering the volume fractions and molar volumes of its components. The density of emulsion formed by a typical slag in oxygen steelmaking conditions with $\phi_g = 0.8$ is found to be between 0.450 to 0.575 kg/m³.

It should be noted that the trajectory of the droplets in the emulsion is included in the current work. This is done through ballistic droplet motion model[24] wherein trajectories of the ascending (into the emulsion zone) and descending (back into the metal bath) motion of metal droplets are predicted and the decarburization occurring during this time period is also accounted for in addition to the decarburization during the bloating period.

III. MODEL ASSUMPTIONS

The residence time and decarburization rate of metal droplets are predicted using an industrial data reported by Cicutti et al.[6,48] for 200-t LD-LBE oxygen steelmaking process. Table I shows the operating conditions of the process. Oxygen is blown through a six-nozzle lance with a flow rate of 10.33 Nm³/s whereas inert gas mix of Ar/N₂ is blown with a flow rate of 0.0416 Nm³/s. 30×10^3 kg of scrap is charged to the process. The composition of slag and hot metal was analyzed by sampling them during the blow and at the end of blow. The following assumptions are made in the model based on this industrial data.

1. Time step Δt of 0.001 seconds is selected for the simulations.
2. The temperature of metal droplet is equal to instantaneous bath temperature and it remains constant during its residence in the emulsion.
3. All the droplets ejected at each time step are assumed to have the same residence time for a defined droplet size.
4. The internal and external CO gas generation compete for oxygen, after the onset of internal gas generation. No constraint is imposed on either of these two reactions and the relative rates of the reactions are calculated separately at the same time.
5. The droplet size distribution is not included in the current work. The droplet size is assumed to be 2×10^{-3} m. This value is valid for industrial data[48] and similar assumption was also made by the previous models.[20,22,49]
6. The initial carbon content of the metal droplet is equal to the bulk carbon content of the liquid metal. The measured values of bulk carbon content of the liquid metal and FeO content of slag were taken as input data for droplet and slag compositions at various times of the blow.

Hot Metal Charged	170×10^3 kg
Scrap Charged	30×10^3 kg
Oxygen Flow Rate	10.33 Nm³/s
Number of Nozzles	6
Lance Height	1.8 to 2.5 m
Initial Hot Metal Temperature	1623.15 K
Tapping Temperature	1923.15 K

7. Metal droplets are dense and have oxygen concentration of 0.02 wt pct (200 ppm) when they are initially ejected into the emulsion zone.

8. In the original model, correction factor (ψ) of 0.023 was used. Even though further work is required for a more rigorous theoretical explanation of the homogeneous nucleation, correction factor has been modified for a range of temperature applicable to oxygen steelmaking conditions. The values for correction factor varied between 0.021 and 0.026. This variation is determined based on model validation against experimental data which is discussed later in section V.A. The value for correction factor equals 0.026 for bath temperatures up to 1813.15 K, whereas equals 0.024 when temperature ranges between 1813.15 K and 1853.15 K. It is 0.021 for temperatures greater than 1853.15 K. It should be noted that in the slags with low FeO content (< 10 pct), the value of (ψ) is expected to decrease.[17] This might be related to the lower nucleation barrier for CO gas formed at the slag–metal interface. However, it is established that there is no bloating behavior of a droplet observed in slags with low FeO content. Therefore, any potential effect of FeO content on the value of (ψ) is not included in this study.

9. The value of slag phase mass transfer coefficient k_s was taken to be 1.5×10^{-4} m/s considering a high basicity value of BOF slag (> 1.2) throughout the blow. This is a reasonable value since Gu et al.[15] have evaluated values ranging from 0.92 to 1.18 $\times$ 10^{-4} for slag basicity of 0.9. The value of mass transfer coefficient in slag could be higher with the progress of the blow, as temperature and the basicity of slag will increase due to increased flux dissolution. An increase in k_s would increase oxygen supply from slag to metal droplet and lead to earlier onset of internal nucleation; however, there will be negligible effect of final carbon content. This is due to the fact that the internal nucleation ceases when the activity of carbon (h_C) decreases beyond a certain value.

10. The bloating behavior of droplets is not affected by the external decarburization because CO gas bubbles generated stays on the surface of the droplet for relatively short time and hence the contact time with the metal droplet is limited and these bubbles will negligibly contribute to the change of droplet density. Contrary to this, the internally nucleated CO gas bubbles which stay inside the metal droplet for a

considerable time. Therefore, CO gas generated due to external decarburization is not considered in evaluation of the residence time and the internally generated CO bubbles are assumed to be only source of buoyancy of the metal droplet.

IV. MODEL FORMULATION

The calculation procedure of the proposed model is provided in Figure 2. The blowing conditions such as oxygen flow rate, presumed slag, and metal composition are entered as input data. The slag density and viscosity are then calculated as a function of composition and temperature. The number of droplets is then calculated as a function of blowing conditions as explained elsewhere.[25] Then the fluxes of oxygen and carbon are calculated, followed by the calculation of the instantaneous weight and surface area of metal droplet as well as activities of metal and slag components. At this point, the internal nucleation of CO is thermodynamically unfeasible. So, at this stage, CO formation takes place on the surface of droplet (termed as external decarburization). The non-linear equations for calculating interfacial concentration and activities of species at the metal droplet–slag interface are solved simultaneously. Due to depletion of carbon, supply of oxygen by CO gas generation, the weight and oxygen and carbon content of a metal droplet are updated. After a certain time, the oxygen concentration inside the droplet rises due to oxygen flux from slag. Consequently, the threshold supersaturation pressure is exceeded (refer Eq. [12]), so that homogeneous nucleation of CO bubbles becomes feasible. There is rapid generation of CO bubbles within the droplet leading to decrease in metal droplet density and suspension of metal droplets in the emulsion. With the increase in internal CO generation, there is a simultaneous escape of CO gas from the metal droplet. The instantaneous balance of CO generation and escape rates determines the apparent density of droplet and consequently the residence time of the metal droplet in the emulsion zone. With the knowledge of the residence time of droplet in the emulsion zone, the amount of carbon removed within an individual metal droplet as well as in the emulsion zone can be determined.

V. MODEL VALIDATION

A. CO Gas Generation

In oxygen steelmaking, dynamic changes in composition and temperature of slag and metal bath influence the decarburization rate. For example, when FeO content of slag is lower than 10 wt pct, external decarburization most likely takes place[10,18] on the other hand, internal decarburization will occur for higher FeO contents. In order to explain decarburization reactions more thoroughly, the authors validated the proposed model under various experimental conditions such as FeO content, temperature and sulfur content.
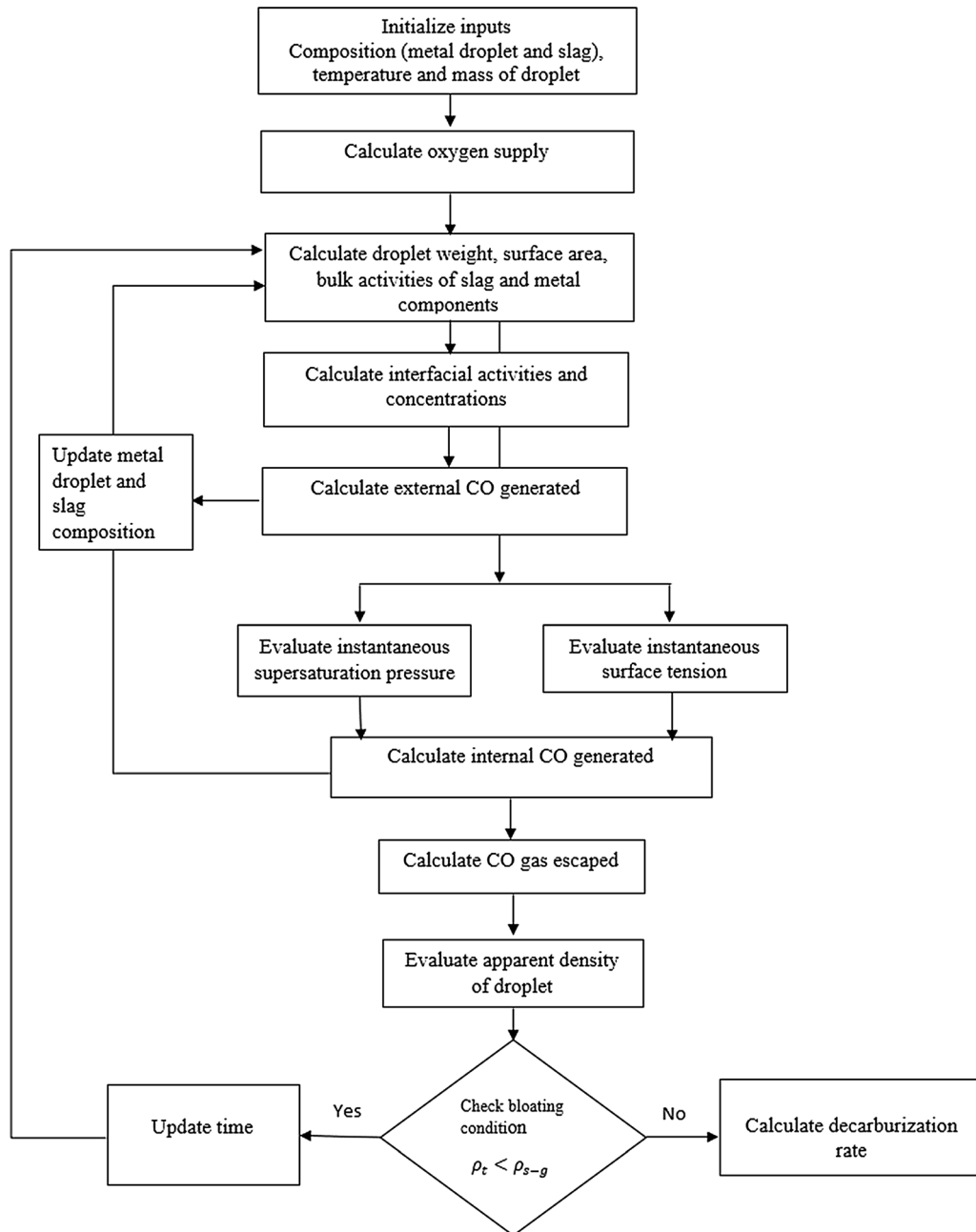
Fig. 2—Algorithm of the decarburization in the emulsion zone model.

In the first case, the model predictions for total CO gas generation are compared with the experimental data reported by Gu et al.[15] They studied the dephosphorization kinetics of metal droplets in ferruginous slag as a function of temperature and sulfur during the decarburization period. The change in droplet size due to external and internal decarburization reactions was observed using X-ray fluoroscopy and the total CO gas evolution was measured by constant volume pressure change measurement technique. The slag composition for all experiments was 35 wt pct SiO_2, 32 wt pct CaO, 17 wt pct Al_2O_3, and 16 wt pct FeO. The carbon content of metal droplet was 2.62 wt pct. The droplet weight was 1 g.

Figure 3 shows the total amount of CO gas generated as a function of experimental temperature and time as well as sulfur content of metal droplets. In the current study, the total CO gas generated is predicted by using Eqs. [17] and [25]. The slag phase mass transfer coefficients were assumed to be 0.92, 1.01 and
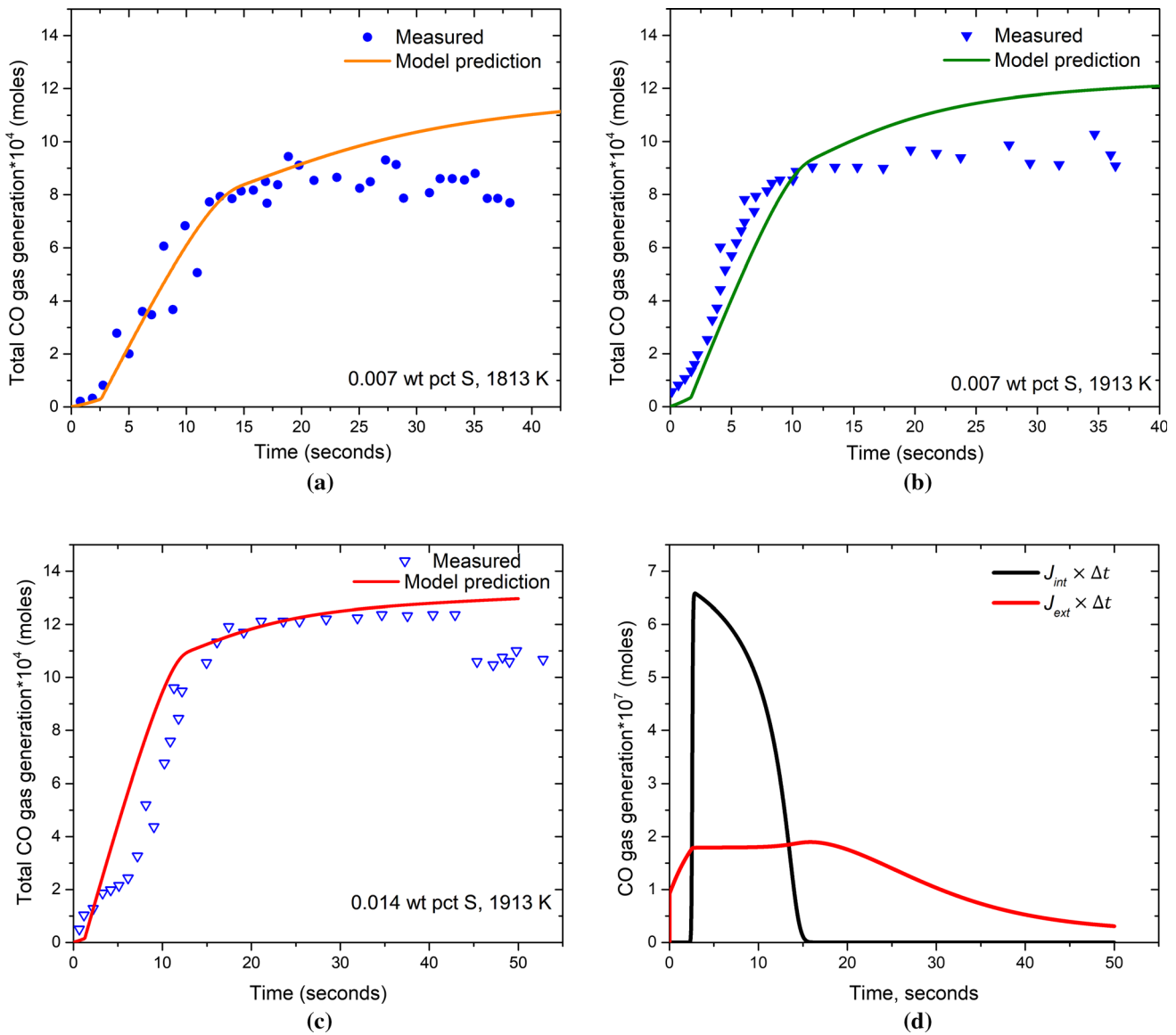
Fig. 3—Comparison of model results for total CO gas generated with measured data by Gu et al.[15] for a metal droplet containing (a) 0.007 wt pct [S] content at 1813 K, (b) 0.007 wt pct [S] at 1913 K, (c) 0.014 wt pct [S] at 1913 K. (d) Comparison of external and internal CO gas generated for a droplet with 0.007 wt pct [S] content at 1813 K, as shown in (a).

1.18×10^{-4} m/s for experiments at 1813, 1853 and 1913 K, respectively. These values were reported by Gu et al.[15] and similar values were used in this study. The solid lines represent the model predictions whereas the points represent the measured data. Total amount of CO gas generated increases with an increase in sulfur content of the droplet. The total CO gas generated for droplets with 0.007 and 0.014 wt pct S are 9×10^{-4} and 1.2×10^{-3} moles, respectively. The model results are consistent with the experimental data reported by the previous researchers except towards the end of decarburization. The over-prediction by the current model is most likely related to local FeO depletion in the foamy slag. When the bloated droplet suspends in the foamy slag, the supply of oxygen would decrease and limit the CO gas generation. In this study, the FeO content in the slag remains constant during the reaction between metal

droplet and slag and the dynamic change in FeO content is not included. However, it should be noted that FeO depletion is not expected to occur during oxygen steelmaking process; therefore, this discrepancy is unlikely to be an issue/limitation for model predictions under oxygen steelmaking conditions.

There are three regimes observed: (1) CO gas generation rate is limited in the first few seconds. During this time, there is insufficient oxygen inside the metal droplet and this leads to formation of CO gas surrounding the metal droplet. This regime is termed as incubation period. (2) There is a significant build-up of oxygen inside the metal droplet leading to substantial generation of CO gas inside the metal droplet. (3) The internal CO gas generation decreases due to a decrease in the activity of carbon. Total CO gas generated increases slightly with time. The contribution of the internal and

external CO gas generated for a metal droplet containing 0.007 wt pct S is compared in Figure 3(d). The model suggests that the external decarburization occurs during the incubation period. Its contribution reaches its maximum value and remains constant when the internal CO gas generation starts. In regime 2, the internal CO gas generation is very rapid and reaches its peak value. As CO gas starts to escape from the metal droplet, the amount of CO gas generated within the droplet decreases. In regime 3, CO gas generation continues outside the metal droplet.

In the second case, the effect of low FeO content was studied. Model results were validated against experimental results of Min and Fruehan.[10] Similarly, their experimental set-up involved X-ray fluoroscopy and a mass flow meter for measuring the rate of gas generation. The metal droplets contained 4.2 wt pct C and 0.001 wt pct S whereas slags contained 7.5 wt pct FeO and CaO/SiO$_2$ ratio of 1. Figure 4 compares the model predictions for CO evolution with measured data as a function of droplet masses (0.78, 1.28, 1.78 × 10^{-3} kg). It should be noted the slag phase mass transfer coefficient used in these particular calculations was 3 × 10^{-5} m/s, and it is based on the work of Wei et al.[50] Min and Fruehan didn't suggest any specific value in their work however they proposed that the slag phase mass transfer coefficient varied between 10^{-4} and 10^{-5} m/s. Further it is established that the mass transfer coefficient of FeO is low for slags with low FeO content at low temperatures.[51] It is observed that there is a constant increase in the amount of CO gas generated as a function of time. This finding agrees well with
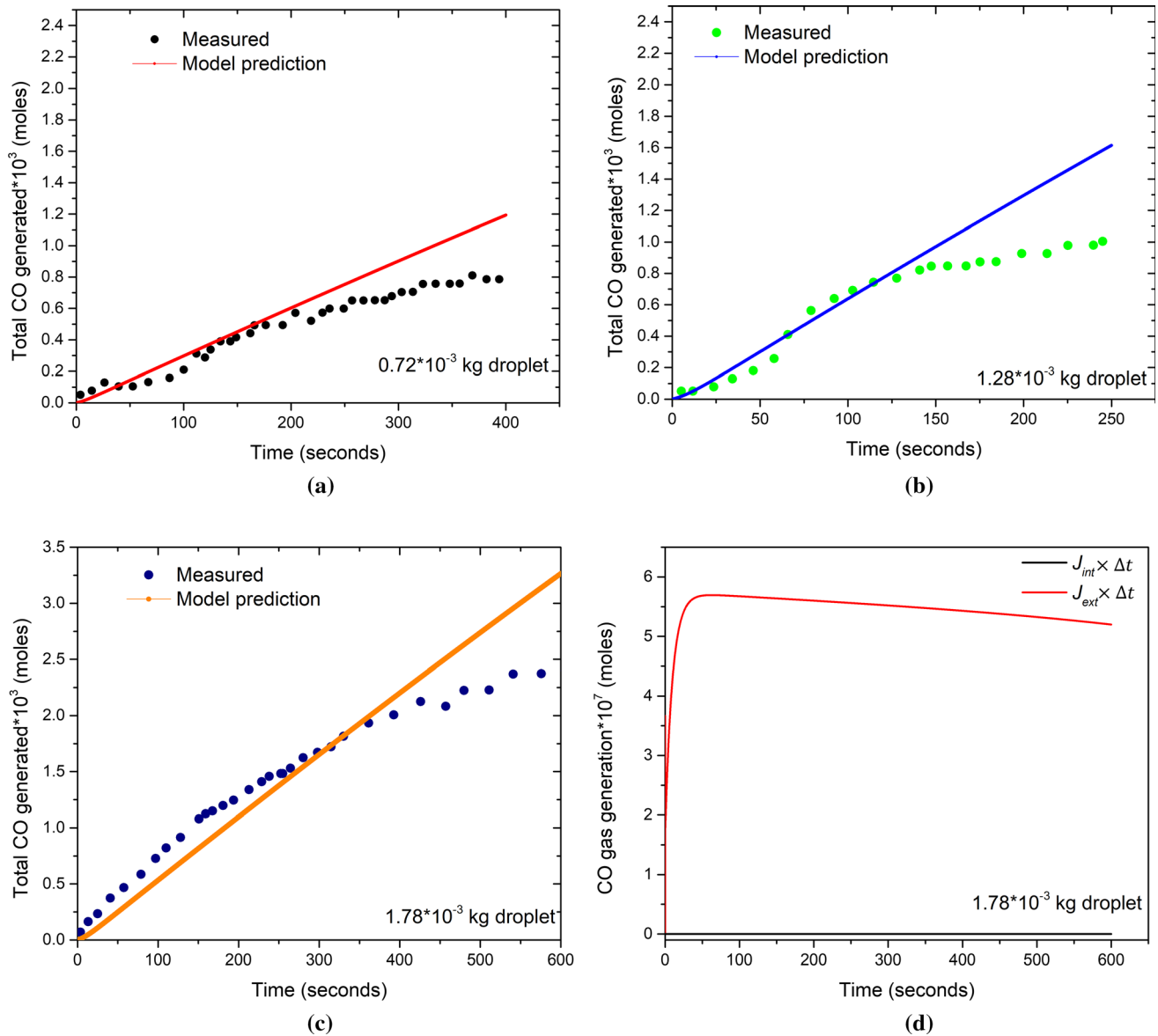

Fig. 4—Comparison of model results for total CO gas generated with experimental data by Min and Fruehan[10] for (a) 0.72 × 10^{-3} kg, (b) 1.28 × 10^{-3} kg, (c) 1.78 × 10^{-3} kg droplet containing 4.2 wt pct [C] and 0.001 wt pct [S] reacted with slag containing 7.5 wt pct FeO, (CaO)/(SiO$_2$) = 1 at 1673 K. (d) Comparison of external and internal CO gas generated for a 1.78 × 10^{-3} kg droplet, as shown in (c).

measured data for the first half of the experiments. Later, there is a disagreement between measured and calculated values. The authors believe that this discrepancy is related to local FeO depletion in the slag as explained for previous case study. The CO gas generated with time increases as the droplet mass increases. This is due to the high amount of carbon within the larger droplet. The contribution of the internal and external CO gas generated for a 1.78×10^{-3} kg metal droplet is compared in Figure 4(d). The model suggests that the external decarburization is very rapid and reaches its peak value in few seconds. It decreases gradually toward the end of the experiment. It is important to note that no internal decarburization is predicted by the model under low FeO contents. This result is consistent with the previous researchers observation wherein Min and Fruehan[10] claimed that the metal droplet was covered by the gas halo during the rapid reaction time, which ranged from 20 to 200 seconds.

Total CO gas generated was 2×10^{-3} moles for a larger metal droplet $(1.78 \times 10^{-3} \text{kg})$. This value was slightly higher than that for a 1×10^{-3} kg metal droplet shown in Figure 3. This is due to the high amount of carbon content of the metal droplet. Even though FeO content in these experiments was low (7 wt pct) and the experimental temperature was 1673 K, the oxygen supply or low temperatures were not limiting factors for total CO gas generated.

B. Residence Times of Droplets

The residence time of droplets is calculated using Eqs. [30], [31] and [32] in the current study. The instantaneous amount of CO gas generated and escaped determines the volume change of a single metal droplet. Therefore, the apparent density of droplet can be calculated if the initial mass of the metal droplet is known. Figure 5 illustrates the calculated apparent

density of 1 g metal droplet containing 0.007 wt pct S at 1853 K by the proposed model using experimental data reported by Gu et al.[15] (described in Section V–A). Based on the change in density of a metal droplet, the droplet behavior can be explained as follows: The apparent density of droplet, ρ_t, is more than that of foamy slag, ρ_{s-g} during incubation period. In regime 2, the apparent density of droplet decreases because of accumulation of CO gas inside it and the droplet suspends in the foamy slag $(\rho_t \leq \rho_{s-g})$. The metal droplet during this stage is termed as 'bloated'.[24] After a certain period of time, the droplet becomes devoid of CO gas as internal nucleation of CO gas ceases and the nucleated CO gas escapes. This leads to an increase in apparent density of droplet again $(\rho_t > \rho_{s-g})$ and the droplet sinks back from foamy slag to dense slag. For model validation against experimental data, the residence time of the droplet is equal to the time when the droplet resides in the foamy slag (regime 2).

The model predictions for residence time of metal droplets are compared with measured data obtained by Gu et al.[15] experiments as shown in Figure 6. The measured data are obtained from available X-ray videos of the experiments.[15] The authors assumed that the measured residence times is the time elapsed between the start of ascending of metal droplet in the dense slag (droplet rises from the bottom of crucible) and the start of descending of metal droplet (droplet reaches the interface between foamy and dense slag). The upper limit/maximum residence time represents the time elapsed between the ascending of the metal droplet and point when the droplet reaches the bottom of crucible. The lower limit/minimum residence time represents the time droplet stays in the foamy slag. The predicted residence times varied between 10.5 to 13 seconds and these values are within the range of observed values.
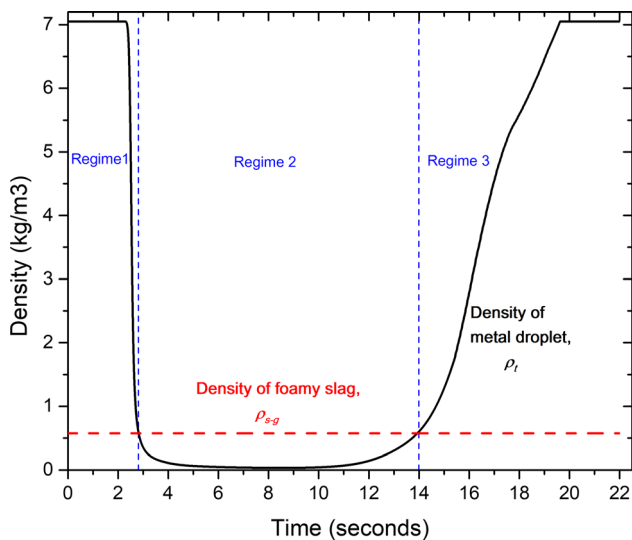

Fig. 5—Change in the apparent density of 1 g droplet containing 0.007 wt pct [S] at 1853.15 K as a function of time.
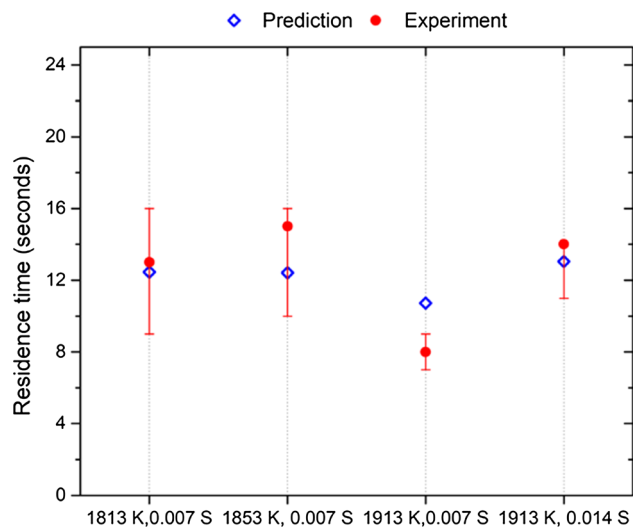

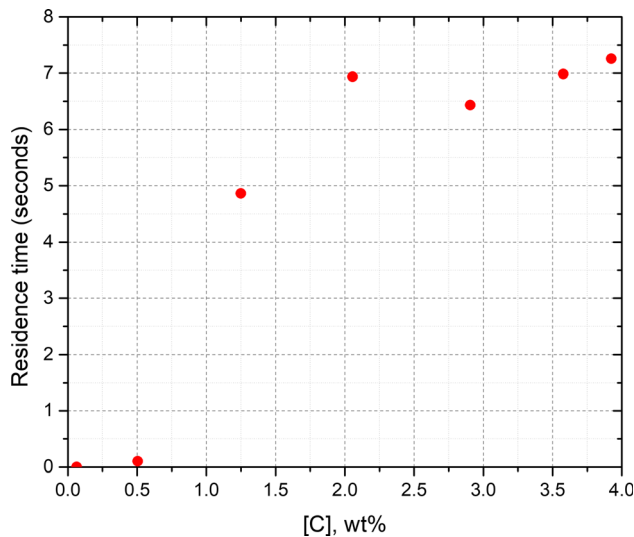Fig. 6—Comparison of model predictions for residence times with the experimental data reported by Gu et al.[15]

Fig. 7—Predicted residence times of metal droplets in the emulsion during the blow.

Fig. 8—Changes in the initial and final carbon contents of metal droplets in the emulsion with respect to blow time.

Table II. List of Measured [C] and (FeO) Contents as a Function of Blowing Time[6,48]

Time, Seconds	[C]	(FeO)
1.89	3.92	33
3.74	3.58	31
5.98	2.91	30
8.90	2.06	17.09
11.28	1.25	11.63
14.37	0.50	18.19
16.97	0.06	22.74

VI. RESULTS AND DISCUSSION

A. Residence Time of Droplets

The model was further studied using the industrial conditions reported by Cicutti et al.[48] The residence time of the droplets is important with regards to the estimation of the extent of decarburization of the droplets. The predicted residence times of 2×10^{-3} m metal droplets during various parts of the blow are presented in Figure 7. The corresponding carbon content of liquid metal [C] and FeO content of slag (FeO) are listed in Table II. In the early part of the blow (0 to 6 mins), the residence time ranges from 6.4 to 7.25 seconds. As the carbon content decreases further with time, the residence time of droplets decreases to 5 seconds and finally merely a second or less. This is due to the fact that the activity of carbon decreases due to the decrease in carbon content within the droplets. This leads to lesser CO gas generation inside the droplets, which is reason for their bloating and spending longer time in the emulsion. It is important to note that the decrease in FeO content does not influence decarburization rate because the oxygen supply from slag is sufficient throughout the oxygen blow. No bloating was predicted by the model for droplets generated beyond 14
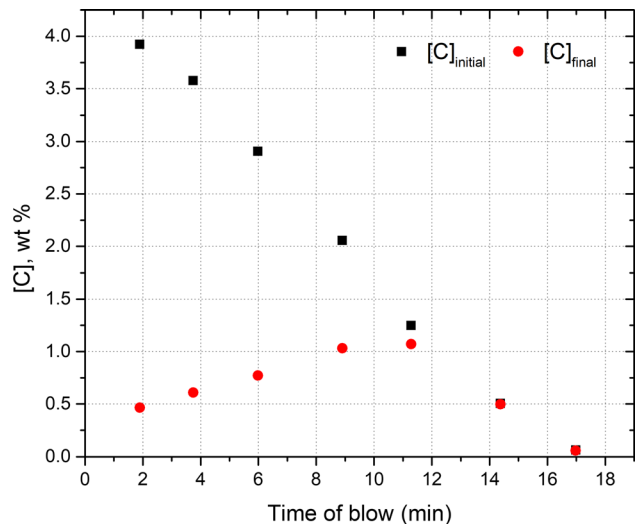
minutes; hence, the residence time was negligible towards the end of blow. The overall trend of residence times and its dependence on [C] and (FeO) contents is similar to those predicted by previous researchers;[2,4,5,19,24] however, shorter residence times are predicted by the current model. The difference between the current model and previous models [19,24] is expected since the calculation procedure is completely changed. In the previous modeling attempts,[19,20] the residence time of a single droplet was calculated based on a ballistic motion of a droplet at vertical and horizontal coordinates within the emulsion. In their attempts, they introduced a correlation to calculate the critical decarburization rate as a function of FeO content of slag. In order to explain the bloating behavior of droplets, they further calculated the apparent density of a single droplet as a function of initial density and the ratio between critical decarburization rate and decarburization rate at a given time step. On the other hand, the current model explains the bloating phenomenon more thoroughly from basic principles by incorporating the internal and external CO gas generation as well as CO gas escape with respect to oxygen supply for any given time step. The current model reduces the empiricism for calculating the residence time of a single droplet.

B. Carbon Content of Metal Droplets

Changes in the carbon content of the metal droplets with respect to blow time are illustrated in Figure 8. The black data points represent the initial carbon content of metal droplets ejected into the emulsion zone whereas red data points represent the final carbon content of metal droplets. This figure shows that the highest carbon removal takes place in the early part of the blow since the residence time of metal droplets is relatively long at this time. Later, it decreases gradually as residence times of metal droplets decrease. Accordingly, the final carbon content increases from 0.45 to 1.11 wt pct during the first half of the blow. The predicted final carbon

contents of the droplets in the emulsion are within the range of values (for sampled droplets) measured by Cicutti et al.[48] during various times of the blow. The observations reported for various blows in an 6-t pilot plant converter[52] are similar, wherein the extent of decarburization (or the difference between carbon contents of the bath and emulsion droplets) decreases with the progress of the blow. This behavior stems from the fact that internal CO gas nucleation strongly depends on the activity of carbon, oxygen, and sulfur (as inferable from Eqs. [12], [22], and [26]). The carbon content [C] and activity h_C decrease during the blow as well as during the residence time of an individual droplet. Carbon being more abundant impurity in liquid metal affects the activities of oxygen and sulfur. During the early part of the blow, high carbon content leads to high activity of sulfur (h_S) as carbon and sulfur have highly positive interaction parameters with respect to each other. Higher values of h_S lead to a greater depression in surface tension of liquid metal thus leading to a higher CO gas nucleation as represented in Eq. [22], $J_s \propto \exp(-\sigma^3)$. This leads to a higher carbon removal in the early part of the blow and thus lower final carbon contents in metal droplets. Furthermore, the analysis of Eq. [22] shows that J_s is inversely proportional to the exponential of the supersaturation pressure squared, ΔP_{CO}^{int}. The activities of carbon (h_C) and oxygen (h_O) and equilibrium constant K_{CO} affect ΔP_{CO}^{int} (refer Eq. [12]). Carbon and oxygen have negative interaction parameters with each other with the progress of blow so h_C decreases while h_O increases. There is a marginal change in the ΔP_{CO}^{int} for various times of the blow and hence a marginal effect on the nucleation of CO gas bubbles within a single droplet (refer Eq. [12]). This indicates that decarburization reaction is mainly limited by the initial carbon content of metal droplet ejected into the emulsion zone.

The authors investigated the effect of droplet size distribution on the residence time of the droplets and decarburization rates. The model predicts that the residence time of droplets will decrease with a decrease in droplet size. However, the amount of carbon removed from a single droplet will be slightly affected. In the early part of the blow, the total decarburization rate in the emulsion will be similar regardless of droplet size and total amount of droplet generated would be more important than the size of the droplets. In the later part of the blow, the decarburization rate is expected to increase only for small droplets (< 0.001 m). This result implicates that controlling droplet size distribution as a function of oxygen blow practice can enhance the decarburization rates in the emulsion zone towards the end of the blow. However, it is certain that greater silicon, manganese and phosphorus refining would occur in the case of smaller droplets as reported by a sampling study of 6-t experimental converter.[52] This is because the refining of these elements occurs at the droplet–slag interface (contrary to decarburization) and smaller droplets would have a larger interfacial area per unit volume. This model will be linked to the process model and the effect of size distribution of droplets will be further studied.

It is important to note that the current work is intended to provide a fundamental description of the bloating behavior and decarburization reaction of a single droplet in the emulsion zone. The effect of silicon and manganese is excluded in this study and would be discussed in subsequent publications. It is expected that the decarburization reaction continues despite the presence of silicon. This is due to the fact that the availability of silicon at interface is limited as compared to carbon even though silicon oxidation is extremely favorable as compared to that of carbon. Manganese will have a much smaller retarding effect on the kinetics of decarburization reaction.

C. Decarburization Rate in Emulsion Zone

The contribution of decarburization rate in the emulsion zone to overall decarburization rate is studied by comparing model predictions for decarburization rates in the emulsion (kg/min) with the total decarburization rate under the operating conditions reported by Cicutti et al. as given in Figure 9. Total decarburization rate was calculated using the theoretical decarburization rate estimated by Cicutti et al.[48] for a post combustion ratio of 0.10 whereas decarburization in emulsion is calculated using equation 1. In the early part of the blow, the decarburization rate is 174 kg/min followed by lower rates 150 to 159 kg/min during main blow (around 6 to 8 minutes), and eventually falls down to 23 kg/min in the 11th minute of the blow. As discussed in the previous section, the presence of silicon during the early blow might decrease the predicted decarburization rate slightly, until the silicon content decreases to extremely low concentration (< 0.05 wt pct).[53] However, this
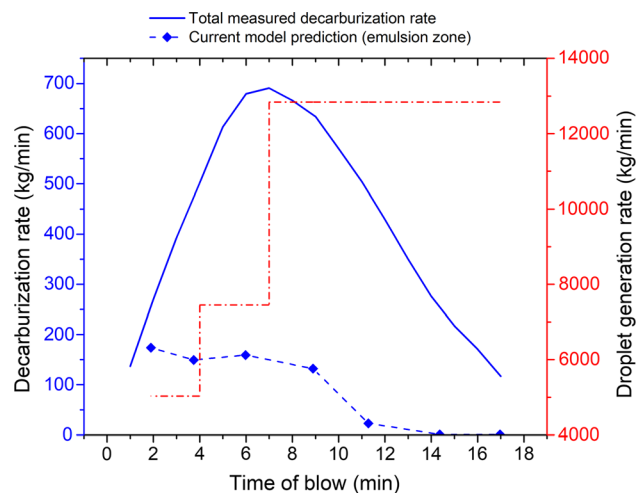

Fig. 9—Comparison of decarburization rate in the emulsion and overall decarburization rate as a function of droplet generation rate and blow time.

effect is not considered in the current model. In the early part of the blow, the decarburization rate in the emulsion zone contributes to 75 pct of the total decarburization rate. Its contribution decreases to 5 pct towards the end of the blow. It is notable that the decarburization per droplet decreases with the progress of the blow, as indicated by the [ΔC] wt pct in Figure 8. However this lower decarburization per droplet is compensated by high droplet generation (blowing time > 5.89 min) wherein droplet generation rises from 5033 to 7450 and 12843 kg/min as shown in Figure 9 and total decarburization does not fall sharply. No significant decarburization is predicted in the emulsion beyond 14 minutes as there is no occurrence of droplet bloating during that period due to low carbon content. It is important to note that the calculations are conducted for a fresh 'set of droplets' generated at each time step and their refining behavior is tracked independently in the calculations. The authors believe that the decarburization rate is strongly dependent on the amount of carbon removed in a single droplet shown in Figure 8 whereas it is slightly influenced by the residence time of the droplet. Therefore, the decarburization rate predictions would be affected slightly. Even though external decarburization continues to occur, the contribution of external decarburization to the overall decarburization is relatively small. This is due to the fact that the residence time of dense droplets is negligible (approximately 0.1 seconds). This model enables to predict the carbon removal within dense and bloated droplets in the emulsion zone. These findings indicate that bloating behavior of droplets is important for refining reactions in the emulsion zone and overall refining kinetics of the process.

The predicted decarburization rate in the emulsion zone shown in the above figure is based on the minimum droplet generation rate derived from the correlation of Subagyo et al.[25] A more recent study by Rout et al.[54] suggests that droplet generation rate is almost five times higher than that of Subagyo et al. Further evaluation of droplet generation rate is required for better understanding of refining kinetics in oxygen steelmaking process. Application of such high droplet generation rate in the current work would increase the decarburization rate in the emulsion zone to an extent that 100 pct of decarburization reaction takes place in the emulsion zone particularly in the early part of the blow and such prediction doesn't reflect the reality. Beyond 11th minute, no significant bloating would be observed and an increase in the number of droplets in the emulsion zone would not lead to increase in any refining after this time. It is quite possible that a considerable fraction of the generated droplets would not reach the emulsion zone (considering their ejection angle and point of origin in cavity). These droplets are splashed within cavities (countercurrent to oxygen jets) and bring about significant refining including the decarburization as well as FeO generation necessary to sustain the emulsion zone refining. Experiments by Koch et al.[55] involving blowing of an oxygen jet on a 50 kg molten Fe-C bath support this claim. The metal droplets "sprayed" from the cavity were sampled at various points of the cross section of the metal sampler during a blow. The authors observed that the "inner" droplets (ejected into the jet) underwent higher refining as compared to the "outer" droplets (ejected into the emulsion zone in radially outward direction). This indicates a possibility of significant contribution of decarburization and other refining reactions in the cavity droplets. The authors believe that the decarburization occurring within the droplets residing in the cavities would be responsible for the residual decarburization which is unaccounted by emulsion zone.

D. Effect of Initial Oxygen Content of Droplet

The instantaneous oxygen content is a function of [Fe]-[O]-(FeO) and [C]-[O]-CO equilibrium and the degree of bottom stirring. The increase in turbulence of bath caused by bottom stirring improves the homogeneity of the bath and causes a fall in its oxygen content (and hence the droplets). The oxygen content of metal bath rises during the initial part of the blow, is almost constant during the middle blow and rises significantly towards the end of the blow. The effect of initial dissolved oxygen content of a metal droplet of size 2×10^{-3} m on the onset of bloating is presented in Figure 10. The initial oxygen content varied from 0.02 to 0.1 wt pct. The model predicts that an increase in initial oxygen content would reduce time for the onset of bloating (the time when $\rho_t \leq \rho_{s-g}$) slightly. This is due to the fact that supersaturation of CO gas is reached in a shorter time. However there is a negligible effect of initial oxygen content on the decarburization rate. This calculation is repeated for droplets ejected at different blow time. There is no noticeable change on the onset of bloating of droplets and total decarburization rate in the emulsion. This indicates that model assumption is suitable for predicting decarburization rates under
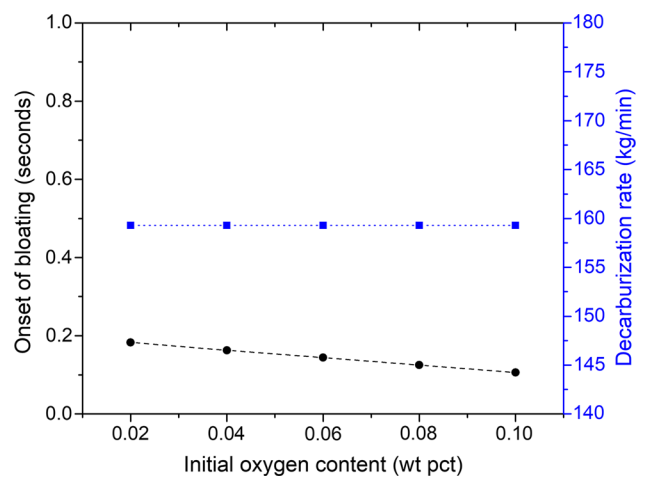

Fig. 10—Effect of initial dissolved oxygen content on onset of droplet bloating and decarburization rate (droplet size 2×10^{-3}m, ejection time: 5.89 min).
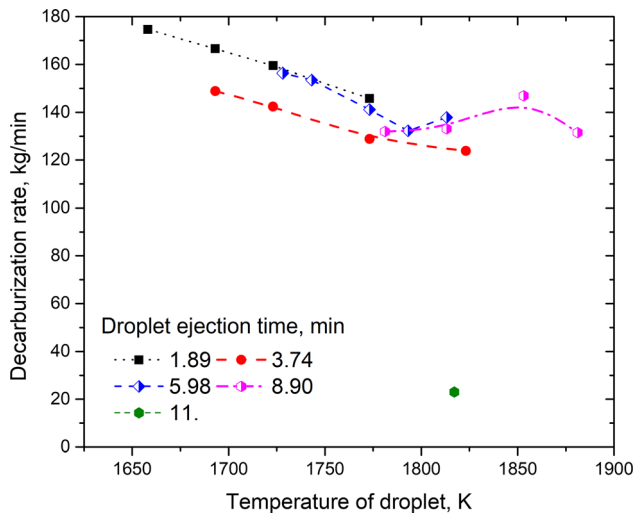
Fig. 11—Effect of droplet temperature on the total decarburization rate in the emulsion zone as a function of blow time.

oxygen steelmaking operating conditions and dissolved oxygen content within the metal droplet can be kept constant.

E. Effect of Temperature of Droplet

In this work, the droplet temperature was assumed to be equal to the instantaneous bath temperature. The effect of droplet temperature (as compared to the bath temperature) on decarburization rates in the emulsion zone is presented as a function of ejection time of metal droplets in Figure 11. The first prediction for each series is the value assumed as base case followed by an increase in temperature of 100 to 200 K. The predicted decarburization rates fall slightly with an increased in temperature up to 1813.15 K, but increase slightly with further decrease in temperature. The initial decrease is caused due to exothermic nature of the decarburization reaction. Thereafter (i.e. above 1813.15 K) slight increase is due the effect of change in value of correction factor ψ. It is constant and equal to 0.026 for calculations below 1813.15 K. Subsequently the value of ψ increases to 0.024 for temperatures up to 1853.15 K and 0.021 for higher droplet temperatures. As explained in the assumption section, 'ψ' is surface tension modifying parameter. Hence, a lower value of ψ entails a higher internal CO gas generation (refer Eq. [22]).

Recent work by Rout et al.[23] attempted to predict the dynamic temperature of metal droplets by assuming the droplet temperature to be equal to impact zone temperature, and it being cooled to temperatures between 1800 K to 2000 K. In their work, the impact zone temperature was approximately 2300 K. Even though droplet temperature would be higher than the instantaneous bath temperature when it enters the emulsion zone, the extent of absorption of heat by the metal droplet during the short period is difficult to measure and not available in the open literature. Therefore a detailed phenomenological heat transfer model incorporated with high temperature experiments will be beneficial for better prediction of droplet

temperature thereby decarburization rates in the emulsion zone. It should be important to mention that these calculations are done with same values of slag phase mass transfer coefficient $(1.5 \times 10^{-4} \text{m/s})$. However this value is likely to increase with an increase in temperature which would counteract the decrease in decarburization. The authors believe that the assumption of droplet temperature is reasonable for the current knowledge. Further studies are required to evaluate the temperature of droplet.

VII. CONCLUSION

A mathematical model is developed to study the decarburization reaction within a single droplet and validated against experimental data available in open literature. Then the residence time and decarburization rate of a single droplet and total decarburization rate in the emulsion are predicted using industrial data reported by Cicutti et al.[6,48] Some significant conclusions of the current model are as follows:

- The bloating behavior of metal droplets in the emulsion was represented theoretically by incorporating internal CO gas generation and CO gas escape. The authors believe that this study is the most scientifically rigorous treatment of bloating behavior of droplets in open literature.
- This model enables the prediction of carbon removal within dense and bloated droplets in the emulsion zone. In the first half of the blow, the droplets become bloated and their residence times range between 6 to 7.5 seconds as the initial carbon content of metal droplets is relatively high. Later in the blow, there is limited bloating (hence small residence time) when carbon content is below 1 wt pct as the activity of carbon decreases. Therefore, droplets remain dense. These results indicate that the residence time of droplets in emulsion is more dependent on the carbon content of droplets as long as FeO content in the slag is not excessively low (below 8 to 10 wt pct).
- The predicted decarburization rate in the emulsion zone is approximately 5 to 75 pct of total decarburization for the industrial operation of Cicutti et al.[6,48] This represents a contribution of 20 pct of total carbon removal using a defined droplet generation rate prescribed by Subagyo et al.[25] approach. The decarburization rate decreases with the progress of the blow and the increase in droplet generation does not adequately compensate for low decarburization per droplet. It is negligible towards the end of the blow (> 14 minutes).
- The current model provides a better understanding of decarburization reaction and confirms the importance of the presence of bloated droplets in the emulsion zone. However, the effect of variations in lance height and oxygen flow rate on the decarburization rate in cavity and emulsion zones remains as future work. These parameters have significant influence on the droplet generation rate, droplet size distribution thereby decarburization rate. Incorporation of this

model into the process model and validation of the process model is essential to help steelmakers gain a better understanding of the process and further optimize/control the industrial operations.

- The initial oxygen content of metal droplets has a minor effect on the onset of internal decarburization and a negligible effect on the decarburization rate. This makes employment of a higher bottom stirring rate favorable rather than an impediment to decarburization in emulsion zone.
- The increase in temperature of droplet reduces the decarburization rate.

APPENDIX A

Calculation of Interfacial Activities of Metal Droplet Components

The activity coefficients for carbon and oxygen can be calculated by taking into account the interaction parameters of carbon, oxygen, and sulfur.

$$\log f_C^r = e_C^C[\text{wt pct} C]^r + e_C^O[\text{wt pct} O]^r + e_C^S[\text{wt pct} S]^r \quad [A1]$$

$$\log f_O^r = e_O^C[\text{wt pct} C]^r + e_O^O[\text{wt pct} O]^r + e_O^S[\text{wt pct} S]^r \quad [A2]$$

The Henrian activities of carbon and oxygen are defined by,

$$h_C^r = f_C^r[\text{wt pct} C]^r \quad [A3]$$

$$h_O^r = f_O^r[\text{wt pct} O]^r \quad [A4]$$

Evaluation of Mole Fraction and Activity of (FeO)

The mole fraction of FeO at the droplet–slag interface is defined by the following equation

$$X_{FeO}^r = \frac{(\text{wt pct FeO})^r}{M_{FeO}\left(\frac{\text{wt pct FeO}^r}{M_{FeO}} + \frac{\text{wt pct SiO}_2^r}{M_{SiO_2}} + \frac{\text{wt pct MnO}^r}{M_{MnO}}\right)} \quad [A5]$$

The Raoultian activity of FeO at the interface can be defined by,

$$a_{FeO}^r = \gamma_{FeO} X_{FeO}^r \quad [A6]$$

Balance of Supply and Consumption of Oxygen at the Interface

The equilibrium constant for decarburization reaction is defined as

$$K_{CO} = \frac{P_{CO}^{\text{ext}}}{h_C^r h_O^r} \quad [A7]$$

The value of P_{CO}^{ext} is taken to be equal to 1.5 atm (equal to the pressure of the furnace).

$$K_{FeO} = \frac{a_{FeO}^r}{h_O^r} \quad [A8]$$

The Eqs. [A7] and [A8] can be rearranged in terms of h_O^r and combined to arrive at the following equation

$$\frac{K_{FeO}}{a_{FeO}^r} = \frac{K_C h_C^r}{P_{CO}}. \quad [A9]$$

NOMENCLATURE

A_d	Surface area of a metal droplet, (m^2)
a_{FeO}	Raoultian activity of FeO in slag $(-)$
e_j^i	First order interaction parameter, of solute j on i
f_C, f_O, f_S	Henrian activity coefficients of carbon, oxygen, and sulfur, respectively
h_C, h_O, h_S	Henrian activities of carbon, oxygen, and sulfur, respectively
J_C, J_{FeO}, J_O	Flux of carbon, oxygen, and FeO towards metal droplet–slag surface, $\left(\frac{\text{moles}}{\text{s}}\right)$
J_{ext}, J_{int}	External and internal CO generation rates respectively, $\left(\frac{\text{moles}}{\text{s}}\right)$
J_{esc}	Net escaped moles of CO gas at a given time step, (moles)
J_s	Nucleation rate, $\left(\frac{\text{nuclei}}{\text{m}^3 \cdot \text{s}}\right)$
K_{CO}, K_{FeO}	Equilibrium constants for CO formation and FeO dissociation reaction
K_O, K_S	Adsorption coefficients of the oxygen and sulfur $(-)$
k_s, k_m	Slag and metal phase mass transfer coefficient, $\left(\frac{\text{m}}{\text{s}}\right)$
$\vec{k}, \overleftarrow{k}$	Forward and backward reaction constants of FeO dissociation reaction $(-)$
m_d	Mass of metal droplet, (kg)
N_{CO}	Net retained moles of CO gas within a metal droplet, (moles)

$P_{CO}^{ext}, \Delta P_{CO}^{int}$ — Supersaturation pressure for external (droplet surface) and internal CO gas generation (atm)

$t_{inst}, t_{res}, \Delta t$ — Instantaneous time, residence time, time step, respectively (seconds)

Δt_e — Time interval during which the emulsion zone decarburization is being evaluated

V_o — Initial volume of metal droplet, (m^3)

GREEK SYMBOLS

θ_S — Fraction of surface area poisoned by sulfur $(-)$

ρ_t, ρ_d — Apparent and initial density of metal droplet $\left(\dfrac{kg}{m^3}\right)$

$\rho_g, \rho_s, \rho_{s-g}$ — Densities of gas, slag, and emulsion, respectively $\left(\dfrac{kg}{m^3}\right)$

σ, σ_{metal} — Surface tension of metal, $\left(\dfrac{N}{m}\right)$

ϕ_g — Volume fraction of CO gas in the emulsion

ψ — Correction factor to the surface tension of the metal $(-)$

SUBSCRIPTS/SUPERSCRIPTS

r — Slag–metal interface

$s - g$ — Emulsion

REFERENCES

1. H.W. Meyer, W.F. Porter, G. Smith, and J. Szekely: *J. Met.*, 1968, vol. 20, pp. 35–42.
2. J. Schoop, W. Resch, and G. Mahn: *Ironmak. Steelmak.*, 1978, vol. 2, pp. 72–79.
3. R.C. Urquhart and W.G. Davenport: *Can. Metall. Q.*, 1973, vol. 12, pp. 507–16.
4. P. Kozakevitch: *J. Miner. Metal Metar. Soc.*, 1969, vol. 22, pp. 57–68.
5. D.J. Price: in *Process Engineering of Pyrometallurgy Symposium*, The Institution of Mining and Metallurgy, London, 1974, pp. 8–15.
6. C. Cicutti, M. Valdez, T. Pérez, R. Donayo, and J. Petroni: *Lat. Am. Appl. Res.*, 2002, vol. 32, pp. 237–40.
7. E.W. Mulholland, G.S. Hazeldean, and M. Davies: *J. Iron Steel Inst.*, 1973, vol. 211, pp. 632–39.
8. T. Gare and G.S. Hazeldean: *Ironmak. Steelmak.*, 1981, vol. 4, pp. 169–81.
9. H. Gaye and P.V. Riboud: *Metall. Trans. B*, 1977, vol. 8, pp. 409–15.
10. D.J. Min and R.J. Fruehan: *Metall. Trans. B*, 1992, vol. 23B, pp. 29–37.
11. C.L. Molloseau and R.J. Fruehan: *Metall. Mater. Trans. B*, 2002, vol. 33B, pp. 335–44.
12. E. Chen: Ph.D Thesis, McMaster University, 2011.
13. E. Chen and K.S. Coley: *Ironmak. Steelmak.*, 2010, vol. 37, pp. 541–45.
14. M.D. Pomeroy: MASc Thesis, McMaster University, 2011.
15. K. Gu, N. Dogan, and K.S. Coley: *Metall. Mater. Trans. B*, 2017, vol. 48B, pp. 1–18.
16. K. Gu, N. Dogan, and K.S. Coley: *Metall. Mater. Trans. B*, 2017, vol. 48B, pp. 2343–53.
17. K.S. Coley, E. Chen, and M. Pomeroy: in *Proceedings of the Extraction and Processing Division Symposium on Pyrometallurgy in Honor of David G.C. Robertson*, P.J. Mackey, E.J. Grimsey, R.T. Jones, and G.A. Brooks, eds., 2014, pp. 289–302.
18. H. Sun and G. Zhang: in *3rd International Congress on Science ans Technology of Steelmaking*, 2005, pp. 257–68.
19. N. Dogan, G.A. Brooks, and M.A. Rhamdhani: *ISIJ Int.*, 2011, vol. 51, pp. 1093–1101.
20. N. Dogan: Ph.D Thesis, Swinburne University, 2011.
21. R. Sarkar, P. Gupta, S. Basu, and N.B. Ballal: *Metall. Mater. Trans. B*, 2015, vol. 46B, pp. 961–76.
22. B. Rout, G. Brooks, M.A. Rhamdhani, Z. Li, F.N. Schrama, and J. Sun: *Metall. Mater. Trans. B*, 2018, vol. 49B, pp. 537–57.
23. B.K. Rout, G. Brooks, M. Akbar Rhamdhani, Z. Li, F.N.H. Schrama, and A. Overbosch: *Metall. Mater. Trans. B*, 2018, vol. 49B, pp. 1022–33.
24. G. Brooks, Y. Pan, Subagyo, and K.S. Coley: *Metall. Mater. Trans. B*, 2005, vol. 36, pp. 525–35.
25. G.A. Subagyo and K.S. Brooks: Coley, and G*A. Irons: ISIJ Int.*, 2003, vol. 43, pp. 983–9.
26. G.R. Belton: *Met. Trans. B*, 1976, vol. 7, pp. 35–42.
27. Y. Kawai and Y. Shiraishi: *Handbook of Physico-Chemical Properties at High Temperatures*, Iron and Steel Institute of Japan, Tokyo, 1988.
28. *Thermodynamic Data for Steelmaking*, ed., M. Hino, and K. Ito, eds., *Thermodynamic Data for Steelmaking*, Tohoku University Press, Sendai, 2010.
29. G.K. Sigworth and J.F. Elliot: *Met. Sci.*, 1974, vol. 3, pp. 298–10.
30. E. Shibata, H. Sun, and K. Mori: *Metall. Mater. Trans. B*, 1999, vol. 30B, pp. 279–86.
31. L.A. Baker, N.A. Warner, and A.E. Jenkins: *Trans. Metall. Soc. AIME*, 1967, vol. 239, pp. 857–64.
32. P.A.A. Distin, G.D.D. Hallett, and F.D. Richardson: *J. Iron Steel Inst.*, 1968, vol. August, pp. 821–33.
33. N. El Kaddah and D.G. Robertson: *J. Colloid Interface Sci.*, 1977, vol. 60, pp. 349–60.
34. K. Mor, H. Sun, K. Ga, V. Sahajwalla, and R.D. Pehlke: *ISIJ Int.*, 1999, vol. 39, pp. 25–33.
35. K. Gao, V. Sahajwalla, H. Sun, C. Wheatley, and R. Dry: *ISIJ Int.*, 2000, vol. 40, pp. 301–08.
36. H.S. Levine: *Metall. Trans. B*, 1973, vol. 4B, pp. 777–82.
37. P.G. Bowers, K. Bar-eli, and R.M. Noyes: *J. Chem. Soc. Faraday Trans.*, 1996, vol. 92, pp. 2843–49.
38. S.D. Lubetkin: *Langmuir*, 2003, vol. 19, pp. 2575–87.
39. A.W. Cramb and I. Jimbo: *Steel Res.*, 1989, vol. 60, pp. 157–65.
40. W. Cramb, W.R. Graham, and G.R. Belton: *Metall. Trans. B.*, 1978, vol. 9, pp. 623–29.
41. K. Ogino, S. Hara, T. Miwa, and S. Kimoto: *Trans. ISIJ*, 1984, vol. 24, pp. 522–31.
42. R. Hongbin, M. Suzuk, D.R. Poirier, H. Yin, M. Suzuki, and T. Emi: *ISIJ Int.*, 1998, vol. 38, pp. 229–38.
43. P. Sahoo, T. Debroy, and M.J. McNallan: *Metall. Trans. B*, 1988, vol. 19, pp. 483–91.
44. Y. Chung and A.W. Cramb: *Metall. Mater. Trans. B*, 2000, vol. 31B, pp. 957–71.
45. F.A. Halden and W.D. Kingery: *J. Phys. Chem.*, 1955, vol. 59, pp. 557–59.
46. K.S. Coley and T.X. Zhu: *Private Communication*, Hamilton, Ontario, 2018.
47. Subagyo and G.A. Brooks: *ISIJ Int.*, 2002, vol. 42, pp. 1182–84.
48. C. Cicutti, M. Valdez, T. Perez, J. Petroni, A. Gomez, R. Donayo, and L. Ferro: in *6th International Conference on Molten Slags, Fluxes and Salts*, Stockholm- Helsinki, 2000, p. 367.
49. N. Dogan, G.A. Brooks, and M.A. Rhamdhani: *ISIJ Int.*, 2011, vol. 51, pp. 1086–92.
50. P. Wei, M. Sano, M. Hirasawa, and K. Mori: *ISIJ Int.*, 1993, vol. 33, pp. 479–87.

51. M. Barati and K.S. Coley: *Metall. Mater. Trans. B*, 2006, vol. 37B, pp. 41–49.
52. M.S. Millman, A. Kapilashrami, M. Bramming, and D. Malmberg: *Imphos : Improving Phosphorus Refining*, European Union, Luxemborg, 2011.
53. B. Deo and R. Boom: *Fundamentals of Steel Making Metallurgy*, Pretince Hall International, Upper Saddle River, 1993.
54. B.K. Rout, G. Brooks, Subagyo, M.A. Rhamdhani, and Z. Li: *Metall. Mater. Trans. B*, 2016, vol. 47, pp. 3350–61.
55. K. Koch, J. Falkus, and R. Bruckhaus: *Steel Res. Int.*, 1993, vol. 64, pp. 15–21.